JGR Biogeosciences

RESEARCH ARTICLE
10.1029/2020JG005892

High Heterogeneity in Canopy Temperature Among Co-occurring Tree Species in a Temperate Forest

Koong Yi[1], Jake W. Smith[1], Andrew D. Jablonski[1], Elizabeth A. Tatham[1], Todd M. Scanlon[1], Manuel T. Lerdau[1,2], Kimberly A. Novick[3], and Xi Yang[1]

[1]Department of Environmental Sciences, University of Virginia, Charlottesville, VA, USA, [2]Department of Biology, University of Virginia, Charlottesville, VA, USA, [3]O'Neill School of Public and Environmental Affairs, Indiana University Bloomington, Bloomington, IN, USA

Key Points:
- Canopy temperature variation is closely related to plant hydraulic traits that govern stomatal regulation
- Sensitivity of canopy temperature to changing air temperature and vapor pressure deficit differs significantly among species
- Difference in canopy temperature among species is comparable to the surface temperature variation caused by land cover change

Supporting Information:
- Supporting Information S1

Correspondence to:
K. Yi and X. Yang,
koongyi@gmail.com;
xiyang@virginia.edu

Citation:
Yi, K., Smith, J. W., Jablonski, A. D., Tatham, E. A., Scanlon, T. M., Lerdau, M. T., et al. (2020). High heterogeneity in canopy temperature among co-occurring tree species in a temperate forest. *Journal of Geophysical Research: Biogeosciences*, *125*, e2020JG005892. https://doi.org/10.1029/2020JG005892

Received 16 JUN 2020
Accepted 5 NOV 2020
Accepted article online 27 NOV 2020

Author Contributions:
Conceptualization: Koong Yi
Data curation: Koong Yi
Formal analysis: Koong Yi
Funding acquisition: Todd M. Scanlon, Manuel T. Lerdau, Kimberly A. Novick, Xi Yang
Investigation: Koong Yi, Jake W. Smith, Andrew D. Jablonski, Elizabeth A. Tatham
Methodology: Koong Yi, Kimberly A. Novick
Project administration: Xi Yang
Resources: Todd M. Scanlon, Manuel T. Lerdau, Xi Yang
Supervision: Xi Yang
Validation: Koong Yi, Todd M. Scanlon, Manuel T. Lerdau, Kimberly A. Novick, Xi Yang
Visualization: Koong Yi
Writing – original draft: Koong Yi
(continued)

Abstract Trees regulate canopy temperature (T_c) via transpiration to maintain an optimal temperature range. In diverse forests such as those of the eastern United States, the sensitivity of T_c to changing environmental conditions may differ across species, reflecting wide variability in hydraulic traits. However, these links are not well understood in mature forests, where T_c data have historically been difficult to obtain. Recent advancement of thermal imaging cameras (TICs) enables T_c measurement of previously inaccessible tall trees. By leveraging TIC and sap flux measurements, we investigated how co-occurring trees (*Quercus alba*, *Q. falcata*, and *Pinus virginiana*) change their T_c and vapor pressure deficit near the canopy surface (VPD_c) in response to changing air temperature (T_a) and atmospheric VPD (VPD_a). We found a weaker cooling effect for the species that most strongly regulates stomatal function during dry conditions (isohydric; *P. virginiana*). Specifically, the pine had higher T_c (up to 1.3°C) and VPD_c (up to 0.3 kPa) in the afternoon and smaller sensitivity of both ΔT ($=T_c - T_a$) and ΔVPD ($=VPD_c - VPD_a$) to changing conditions. Furthermore, significant differences in T_c and VPD_c between sunlit and shaded portions of a canopy implied a non-evaporative effect on T_c regulation. Specifically, T_c was more homogeneous within the pine canopy, reflecting differences in leaf morphology that allow higher canopy transmittance of solar radiation. The variability of T_c among species (up to 1.3°C) was comparable to the previously reported differences in surface temperature across land cover types (1°C to 2°C), implying the potential for significant impact of species composition change on local/regional surface temperature.

1. Introduction

One of the important roles of forests in the climate system is the modulation of energy and water exchanges between land and the atmosphere, which can modify surface temperature and influence local/regional air temperature (Alkama & Cescatti, 2016; Novick & Katul, 2020; Zhao & Jackson, 2014). Recently, substantial efforts have been made to improve understanding of this process in order to clarify the direction and sensitivity of surface temperature change, which will enable a more holistic perspective on the climate mitigation potential of forests. At spatial scales larger than stand/ecosystem scale, the surface temperature is controlled by surface-atmosphere feedbacks (Monteith & Unsworth, 2014). At finer scales (i.e., individual tree scale), canopy temperature (T_c), which is the surface temperature for an individual tree, is a result of the energy balance between net radiation, latent heat flux, and sensible heat flux. These processes are controlled by environmental factors including air temperature, humidity, wind speed, canopy structure, and evaporative heat loss regulated by plants (i.e., transpiration; Jones, 2004). Given that changes in the canopy structure take place at a relatively long time scale (weeks to months), the sensitivity of T_c is largely dependent on shorter-term changes in environmental conditions and associated plant water regulation (hours to days; Mahan & Upchurch, 1988).

The sensitivity of T_c to changing conditions can vary across species due to the wide range of different hydraulic traits that influence stomatal regulation (e.g., from isohydric to anisohydric; McDowell et al., 2008; Yi et al., 2019). Species-level differences in stomatal conductance, in turn, cause different evaporative cooling effects (i.e., heat loss at the leaf surface during transpiration due to the water phase transition from liquid to vapor) among species. Improved understanding of the species-specific sensitivity of T_c is especially important for areas such as the eastern United States, where tree species composition is highly dynamic. Specifically, in this region, the combined influence of fire suppression, management, and long-term

Writing – review & editing: Koong Yi, Jake W. Smith, Andrew D. Jablonski, Elizabeth A. Tatham, Todd M. Scanlon, Manuel T. Lerdau, Kimberly A. Novick, Xi Yang

climate changes in the twentieth century has led to pronounced shifts in species composition in deciduous forests—from forests dominated by more anisohydric oak species, to forests dominated by more isohydric, non-oak species (Abrams, 2003; Fei et al., 2011; Flatley et al., 2013).

The balance of T_c with changing environmental conditions is also important to the plant itself because virtually all plant functions are sensitive to temperature. Temperature outside the optimal range can reduce carbon assimilation, water regulation, and other metabolic processes, acting as a stress (Berry & Bjorkman, 1980). Differences in T_c among species further imply different evaporative gradients from the leaf to air (vapor pressure deficit, VPD) across species by influencing saturation vapor pressure inside the leaf (Helliker & Richter, 2008), with elevated VPD acting as water stress near the leaf surface (Grossiord et al., 2020). Investigating how hydraulic traits mediate temperature and VPD stress, and the consequences for T_c, will improve the understanding of plant vulnerability to predicted changing climate in the future, which is expected to be warmer and drier in many places (Ficklin & Novick, 2017; Intergovernmental Panel on Climate Change [IPCC], 2018; Novick et al., 2016).

Although there have been a few studies investigating tree T_c across species (e.g., Gimenez et al., 2019; Leuzinger & Körner, 2007; Leuzinger et al., 2010), we still don't know if shifts in hydraulic trait diversity affect T_c in ways that are meaningful for physiological function and local micro-climate. One of the major causes of lacuna is the lack of continuous, high-frequency, long-term monitoring of both T_c and plant water use together. This has been challenging until the recent advance of thermal imaging cameras, or TICs, which can resolve the thermal signature of individual trees. The T_c data in most previous studies utilizing TICs were not continuously collected as part of a long-term monitoring protocol; images were taken by choosing a number of times and days of favorable conditions for measurements (clearness, wind, temperature, etc.), which may only represent limited "normal" conditions. Long-term, continuous observations of T_c over a wider range of environmental conditions provide a valuable opportunity to understand links between canopy temperature and physiological response to changing environmental conditions. Infrared radiometers are widely used for continuous, stand-scale T_c measurements (Blonquist et al., 2009; Gimenez et al., 2019; Greer & Weedon, 2012). However, they are designed to record a single value per field of view (FOV), which makes them poorly suited for measuring individual tree canopies and addressing temperature heterogeneity within a single canopy, which is most likely caused by difference in light abosorption depending on the position and angles of individual leaves. A limited number of recent studies relying on continuous long-term operation of TICs have validated T_c measurements for tree canopies (e.g., Aubrecht et al., 2016; Kim et al., 2016, 2018) and proved the potential of TICs to improve our understanding of the interaction between plant physiology and environmental changes.

Leveraging the recent advancement of TIC technology along with synchronous measurements of sap flux, the aim of this study is (1) to understand how the canopy temperature (T_c) and VPD near the canopy surface (i.e., at the canopy-air interface; VPD_c) are coordinated with species-specific stomatal regulation and (2) to evaluate heterogeneity of T_c within canopy. Our study species are three canopy-dominant species growing in a temperate forest located in the eastern United States—white oak (*Quercus alba* L.), southern red oak (*Quercus falcata* Michx.), and Virginia pine (*Pinus virginiana* Mill.). Specifically, (1) we first identify hydraulic traits of study species by assessing their stomatal responses under different soil moisture conditions, (2) characterize the diurnal pattern of T_c and its deviation from T_a (i.e., $T_c - T_a = \Delta T_{c\text{-}a}$), as well as the corresponding pattern of VPD (i.e., $VPD_c - VPD_a = \Delta VPD_{c\text{-}a}$, where VPD_a is atmospheric VPD), and (3) quantify the sensitivity of $\Delta T_{c\text{-}a}$ and $\Delta VPD_{c\text{-}a}$ to changing environmental conditions for each species in terms of T_a and VPD_a. We then discuss how the sensitivities of $\Delta T_{c\text{-}a}$ and $\Delta VPD_{c\text{-}a}$ are associated with species-specific hydraulic traits. We apply these approaches to two different groups of canopy portions divided by their temperatures—defined as sunlit and shaded canopy portions—to further assess heterogeneity of T_c (sunlit T_c − shaded $T_c = \Delta T_{su\text{-}sh}$) within a single canopy and compare it across species and see if the influence of the evaporative cooling effect would hold for leaves receiving different levels of incoming radiation.

We hypothesize that species that tend to prioritize water conservation by closing stomates at an earlier level of water stress (i.e., isohydric species) will overall have higher canopy temperatures and be associated with lower sensitivity of $\Delta T_{c\text{-}a}$ and $\Delta VPD_{c\text{-}a}$ to changing moisture conditions. On the other hand, species positioned on the other side of hydraulic spectrum (i.e., prioritizing carbon uptake even under water stress by sustaining stomatal openings; anisohydric) will have cooler surfaces and higher sensitivities. We also

hypothesize that pine will have more homogeneous T_c distribution within the canopy (i.e., smaller $\Delta T_{su\text{-}sh}$) than oaks. This is based on a speculation that pine will allow higher canopy transmittance of solar radiation due to its more heterogeneously distributed needles within the canopy than broadleaves (Cescatti, 1998); consequently, pine needles are expected to warm up more evenly during the day.

2. Materials and Methods

2.1. Site Description

The study site (Virginia Forest Research Facility) is located in the footprint of an eddy covariance tower running in central Virginia, USA (37° 55′N 78° 16′W). Mean annual temperature and precipitation are 14.0°C and 1,210 mm (over 90% as rain), respectively (1981–2010 normals). The plant functional type is temperate mixed forest dominated by white oak (*Quercus alba* L.), Virginia pine (*Pinus virginiana* Mill.), southern red oak (*Q. falcata* Michx.), red maple (*Acer rubrum* L.), and tulip poplar (*Liriodendron tulipifera* L.). Their relative dominances (=basal area of a species/basal area of all trees × 100%) within a 500 m radius from the flux tower were 23.6%, 20.0%, 11.9%, 11.5%, and 10.3%, respectively (Chan, 2011). The range of diameter at breast height (DBH) was 2.5 to 81.0 cm, with tree size of second and third quartiles ranging from 4.0 to 15.1 cm. Among the species, Virginia pine (hereafter PV, DBH = 46 cm), white oak (hereafter QA, DBH = 36 cm), and southern red oak (hereafter QF, DBH = 30 cm) were selected as observation targets (one tree for each species) considering their relative abundance, and the position and FOV of the TIC. The heights of the target trees were approximately 25 m. The study period was the growing season of 2019, from mid-July to early October. The soil moisture condition was relatively moist throughout the study period; the volumetric water content (VWC) ranged from 0.25 to 0.45 $cm^3\ cm^{-3}$, and the mean value (±standard deviation) was 0.32 (±0.04) $cm^3\ cm^{-3}$ (see Figure S1 in the supporting information for time series and histogram of VWC).

2.2. Canopy Temperature Measurements Using a Thermal Imaging Camera

A TIC (FLIR A655sc with 45° FOV lens; FLIR Systems, Wilsonville, OR, USA) was installed on the top platform of the flux tower (40 m tall) to monitor temperature of target canopies (see Figure S2 in the supporting information for preliminary outdoor test results before installation). The distance between the TIC and target canopies was approximately 15 m (Figure 1). To protect the TIC from damage and foreign materials and to maintain optimal conditions for operation, the camera was housed in a thermostatically controlled enclosure (S-Type COOLDOME enclosure; Dotworkz Systems, San Diego, CA, USA). Still images of infrared radiation (spectral range: 7.5–14 μm) emitted from the target tree canopies were taken every 10 min throughout the study period. The resolution of the images is 640 × 480 pixels. A single output image (file format: SEQ) stores information of thermal signals for all pixels (640 × 480 = 307,200 pixels total) received by the camera sensor and metadata required for thermal signal correction.

In order to account for atmospheric attenuation of the thermal signal transmitted from the canopies to the camera sensor, we applied the correction suggested by Aubrecht et al. (2016). Here, we only report details about the correction that is unique for our study (see Aubrecht et al., 2016, for more details). Among the parameters required for the correction, sky temperature is measured by a net radiometer installed on the top platform of the tower (CNR4; Kipp & Zonen, Delft, Netherlands). Distance between canopy and camera (=15 m) was estimated based on the dimensions of components in our measurement setup (Figure 1a), including distance of TIC from the ground, tree height, and horizontal distance between tower and trees. Correction was applied for every pixel in the thermal images.

As a proxy of ambient dryness imposed on the canopy, VPD at the canopy surface (VPD_c) was calculated using T_c. The series of equations for calculating atmospheric VPD (VPD_a) is as follows (Equations 1–3):

$$\mathrm{VPD} = vp_{sat} - vp_{air} \tag{1}$$

$$vp_{sat} = \frac{610.7 \cdot 10^{\frac{7.5\,T_a}{237.3\,+\,T_a}}}{1000} \tag{2}$$

$$vp_{air} = \frac{610.7 \cdot 10^{\frac{7.5\,T_a}{237.3\,+\,T_a}}}{1000} \cdot \frac{RH}{100} \tag{3}$$

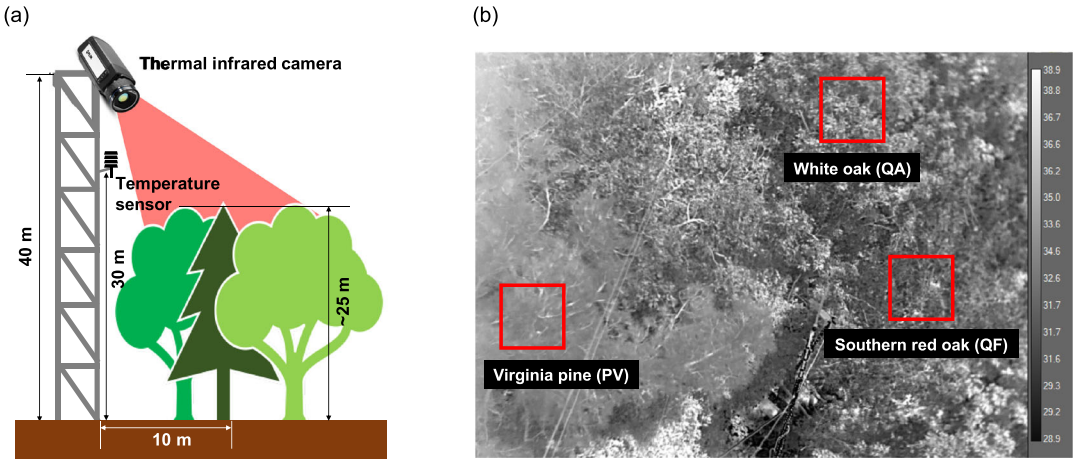

Figure 1. Measurement setup (a) and a sample thermal image taken at 13:00 EST on 8 August 2019 (b). Overlaid red boxes (70 × 70 pixels for each) in the sample thermal image represent regions of interest (ROIs) for different canopies. The spatial resolution is ~2.5 cm. The scale bar in panel (b) indicates surface temperature distribution (unit: °C).

where vp_{sat} is saturated vapor pressure of the air, vp_{air} is actual vapor pressure of the air, and RH is relative humidity. The T_a and RH were measured by a temperature and humidity probe (HMP45; Vaisala, Helsinki, Finland) installed on the tower at the height of 30 m from the ground. To calculate VPD_c, the T_a in the equation for vp_{sat} (Equation 2) was replaced with T_c, such that

$$vp_{sat,\,canopy} = \frac{610.7 \cdot 10^{\frac{7.5\,T_c}{237.3 + T_c}}}{1000} \tag{4}$$

The same RH was used to calculate both VPD_a and VPD_c with the assumption that the differences in mixing of water vapors at the leaf surface (for VPD_c) and in the air near the leaf surface (for VPD_a) were negligible.

Finally, the representative sunlit and shaded T_c for each species were determined by setting a square sample area (i.e., region of interest, ROI) for each canopy (Figure 1). Our definitions of sunlit and shaded portions of a canopy are based on the assumptions that leaves are mainly warmed by light absorption and difference in transpiration rate among the leaves within ROI is negligible. The size of each ROI was 70 × 70 pixels. The ROIs were chosen by visual inspection of images, ensuring pixels of bare ground are not included. The sunlit and shaded T_c were determined in a conservative manner to avoid selecting the portions of extreme T_c only. We assumed that the pixels within the highest 25% of temperatures represent the canopy portions absorbing ample sunlight; T_c from these pixels were averaged to define "sunlit T_c." On the other hand, the pixels within the lowest 50% temperatures were assumed to be T_c of the canopy portions absorbing significantly less sunlight than the sunlit portions; T_c from these pixels were averaged to define "shaded T_c." For these definitions, data collected during daytime from 9 a.m. to 4 p.m. were used. Both sunlit and shaded T_c were converted into hourly data by taking averages of the original data collected every 10 min.

2.3. Sap Flux Measurements

Sap flux densities (J_s, $cm^3\ cm^{-2}\ hr^{-1}$) of the target trees were monitored using a measurement system (HRM30 Sap Flow Sensors and SL5 Smart Logger; ICT International, Armidale, New South Wales, Australia) that adopts the heat ratio method (Burgess et al., 2001). The sap flux sensors consist of three 3.5-cm-long needles inserted into the tree trunk at breast height in a radial direction, with a vertical separation distance of 5 mm; a pair of temperature sensors detect temperature variation and a heater positioned between two sensors generates heat pulses every 10 min. The J_s was measured at a radial depth of 12.5 mm from the epoxy base of the sensors, where thermocouples are positioned, to represent J_s at sapwood area. Correct radial placement of thermocouples was inferred from the sapwood depth of each tree, which

were measured after collecting tree-ring cores. The J_s was originally recorded every 10 min and was converted into hourly data by taking averages of the original data for each species.

To identify hydraulic traits of the study species, we used a diagnostic framework (Equation 7) that combines the concept of soil-plant-atmosphere continuum (SPAC; Equation 5) and a simplified relationship between J_s and g_s (Oren et al., 1999; Equation 6) as follows:

$$J_s(\text{as a proxy of transpiration}) = K(\Psi_S - \Psi_L) \tag{5}$$

$$J_s = g_s \times \text{VPD}_a \tag{6}$$

$$g_s = \frac{K(\Psi_S - \Psi_L)}{\text{VPD}_a} = \frac{K(\Delta\Psi)}{\text{VPD}_a} \tag{7}$$

where K is whole-plant hydraulic conductance, Ψ_S is soil water potential, Ψ_L is leaf water potential, and $\Delta\Psi$ is the difference between Ψ_S and Ψ_L. The contribution of gravitational head loss to $\Delta\Psi$, which is relatively constant over weekly to monthly time scales, is neglected. The equation suggests that the tendency for plants to regulate leaf water potential (Ψ_L) under contrasting soil moisture conditions (Ψ_S) is reflected by stomatal regulation (g_s) and its response to changing VPD_a: Species that tend to conserve water under low Ψ_S by keeping Ψ_L constant (thus rapid decrease in $\Delta\Psi$) would show larger decreases in g_s when soil moisture is generally low (i.e., low Ψ_S), compared to the species that are less conservative in their regulation of Ψ_L. Specifically, we compared g_s-VPD_a (or VPD_c) relationships under two contrasting soil moisture conditions; wet ($\text{VWC} \geq 0.28\ \text{cm}^3\ \text{cm}^{-3}$ within the depth of 30 cm) and dry ($\text{VWC} < 0.28\ \text{cm}^3\ \text{cm}^{-3}$) conditions. Our assumption is that VWC represents the amount of soil moisture trees can access, and the study trees have the same accessibility to the soil moisture (see section 4.1 for limitations of the assumption). The threshold of VWC to define wet and dry conditions was decided after investigating the distribution of VWC during the study period (see Figure S1 in the supporting information for histogram of VWC). Specifically, we set two criteria to determine dry condition: (1) Dry condition is less common condition compared to moderate to wet condition in our site (given $\text{VWC} > 0.25\ \text{cm}^3\ \text{cm}^{-3}$ throughout the study period), and thus, we assume dry condition should not exceed 30% of entire period; (2) dry condition must have at least 100 sampling numbers to avoid uncertainty arising from having low sample numbers. As a result, 28% of data were classified as dry condition and the rest 72% as wet condition. To facilitate comparison of stomatal responses among the study species, the estimated g_s was normalized by dividing g_s-VPD_a curves by the value of g_s at $\text{VPD}_a = 1$ kPa.

2.4. Data Analyses

The species-specific physiological responses (i.e., normalized g_s, $\Delta T_{c\text{-}a}$ ($=T_c - T_a$), $\Delta\text{VPD}_{c\text{-}a}$ ($=\text{VPD}_c - \text{VPD}_a$), and J_s) to changing environmental conditions (i.e., T_a and VPD_a) were assessed based on the data collected during daytime from 9 a.m. to 4 p.m. To clarify the patterns of these relationships, the physiological data were partitioned into discrete bins spanning a range of environmental drivers (e.g., in Figures 5 and 6, each symbol represents a mean value of data points belong to each bin). The widths of the data range for individual bins are not necessarily identical because the size was determined based on the data distribution; every bin was forced to have an equal number of samples (approximately 80) in order to prevent a bias arising from skewed data distribution (e.g., the sample mean from the extreme ends of T_a or VPD_a may not represent the population mean if the sample values are spread out over a wide range and the sample size is small). Difference in $\Delta T_{c\text{-}a}$ or $\Delta\text{VPD}_{c\text{-}a}$ between sunlit and shaded canopy portions (in Figures 5 and 6) was evaluated by using one-way analysis of variance and Tukey post hoc test at a significance level of 0.05 using SPSS Statistics (v.27). The diurnal patterns of plant physiological responses were represented by mean hourly data over the study period.

3. Results

3.1. Species-Specific Hydraulic Traits

All species had a unimodal diurnal pattern of J_s (Figure 2; see Figure S3 in the supporting information for the time series of J_s variation over the entire observation period), linked to the diurnal range of photosynthetically active radiation. The J_s was minimal until early morning, increased until midday, and then decreased gradually, reaching minimal J_s again by sunset. There was a species-specific difference, however, when J_s

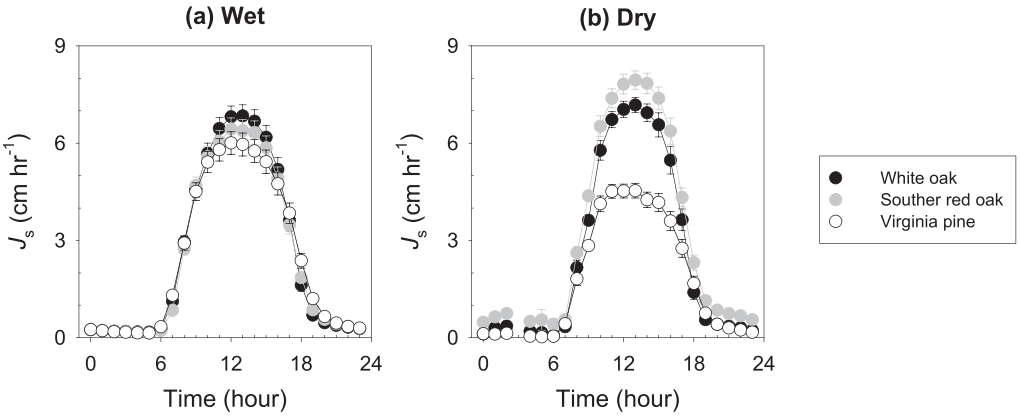

Figure 2. Mean diurnal patterns of species-specific sap flux density (J_s) under wet (volumetric water content [VWC] ≥ 0.28 cm^3 cm^{-3}, a) and dry (VWC < 0.28 cm^3 cm^{-3}, b) conditions (QA: white oak, QF: Southern red oak, and PV: Virginia pine). Error bars represent standard errors of the means (95% confidence).

under different soil moisture (VWC) conditions were compared. While the J_s of PV was substantially decreased under drier conditions (~25% around noon), oaks increased J_s (~5% and ~25% around noon for QA and QF, respectively).

Species-specific differences in stomatal regulation were also evident when the response of g_s to changing VPD was evaluated under contrasting soil moisture conditions (Figure 3). Specifically, g_s of PV under dry conditions was noticeably lower than under wet conditions (Figures 3e and 3f). On the other hand, g_s of QA were very similar in both wet and dry periods (Figures 3a and 3b), while QF had even higher g_s during drier period (Figures 3c and 3d). In addition, g_s response to VPD under wet condition was more sensitive for PV than for other species. Sensitivity of g_s to changing VPD_c (Figures 3b, 3d, and 3f) was not substantially different from the sensitivity to changing VPD_a (Figures 3a, 3c, and 3e), although the range of VPD_c was slightly different from VPD_a which was more prominent for PV: the maximum VPD_a and VPD_c for PV were 4.39 and 4.97 kPa, respectively (Figure 3e vs. Figure 3f).

3.2. Diurnal Patterns of T_c and VPD_c

Mean diurnal patterns of T_c were similar to the pattern of T_a for all species, reaching a minimum temperature around 5 a.m. and maximum around 1 p.m. (Figure 4a; see Figure S4 in the supporting information for T_a and T_c variation over entire observation period). For all species, sunlit T_c was higher than T_a during most of the daytime (from 8 a.m. to 5 p.m.: Figure 4b), up to 0.9°C for QA (peaked at 10 a.m.), 1.6°C for QF (peaked at noon), and 1.5°C for PV (peaked at 3 p.m.). Among the species, PV's T_c warmed more slowly in the morning and cooled more slowly in the afternoon (Figure 4b). Specifically, in the morning, QA (from 7 a.m. to 10 a.m.) and QF (from 7 a.m. to 1 p.m.) had higher sunlit T_c than PV up to 0.9°C and 0.8°C, respectively (both peaked at 8 a.m.). In the afternoon, sunlit T_c of PV was higher than the other species—up to 1.3°C higher than both QA (peaked at 5 p.m.), and QF (peaked at 6 p.m.). There was slight increase in $\Delta T_{c\text{-}a}$ during night (from 9 p.m. to 4 a.m.) across all species, indicating slower cooling of T_c than T_a at night.

Compared to the sunlit T_c, the diurnal variations of the shaded T_c were notably larger across the species (Figure 4c). PV showed lower diurnal variation of shaded T_c than the other species; diurnal variation of the difference between sunlit and shaded T_c was 0.2–1.5°C for QA, 0.2–1.9°C for QF, and 0.3–0.9°C for PV. The difference was highest at 1 p.m. Shaded T_c of QA and QF, unlike the sunlit T_c, were always lower than T_a (up to 0.9°C for QA and 1.2°C for QF, peaked at 7 a.m. and 6 p.m.) throughout the day. On the other hand, PV maintained higher T_c than T_a (up to 0.7°C, peaked at 5 p.m.) at most times except a few hours in the morning (from 6 a.m. to 9 a.m.).

The diurnal patterns of VPD_c for the three species closely followed the patterns of corresponding T_c (Figure 4d). All species had higher sunlit VPD_c than VPD_a during most of the daytime (between 9 a.m. and 5 p.m.), up to 0.2 kPa for QA (peaked at 10 a.m.), 0.4 kPa for QF (peaked at noon), and 0.4 kPa for

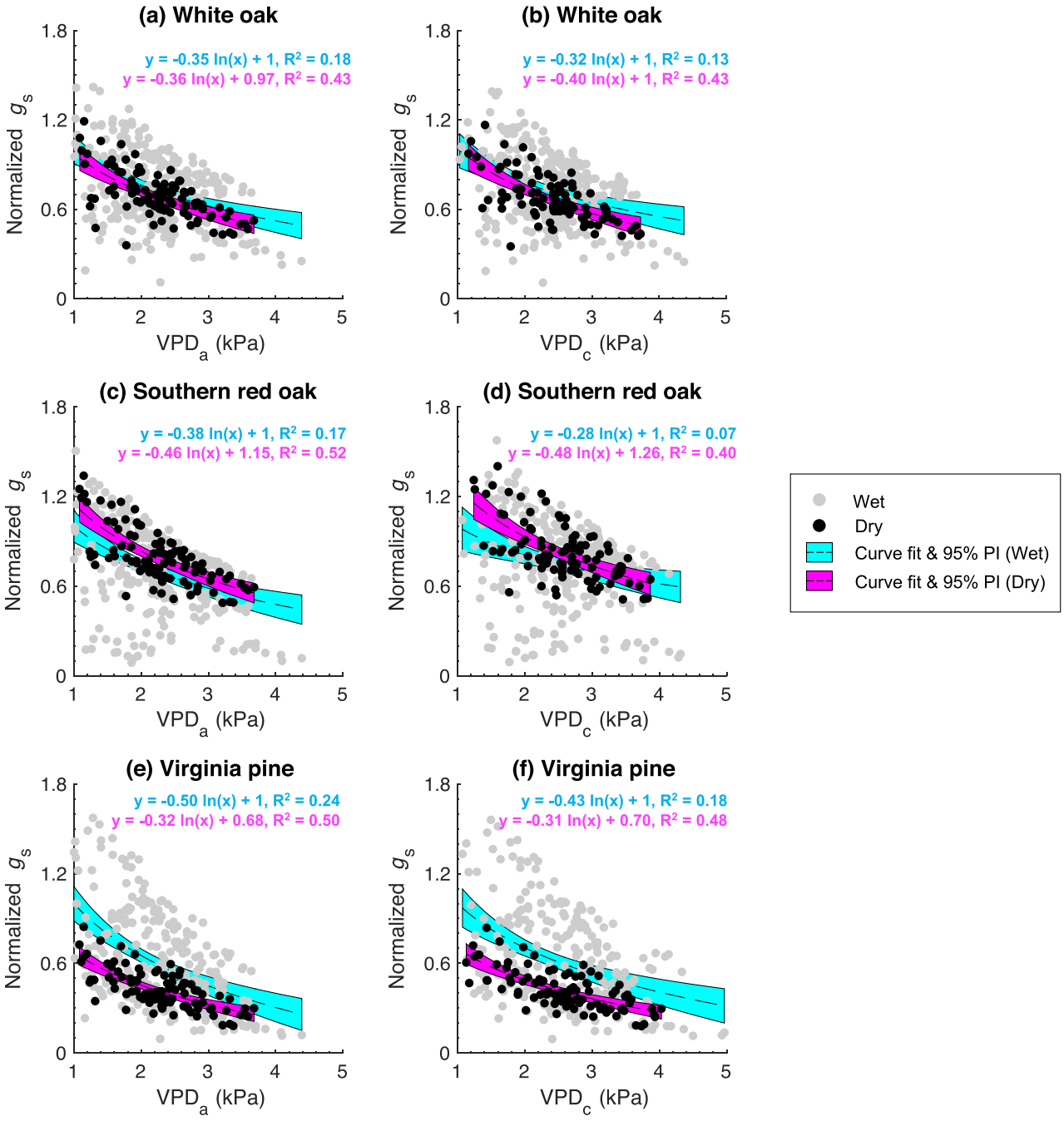

Figure 3. Species-specific relationships between normalized stomatal conductance (g_s) and VPD_a (a, c, e) or VPD_c (b, d, f) under contrasting soil moisture conditions. The g_s values under both wet and dry conditions were normalized by dividing g_s by wet condition g_s at VPD_a or VPD_c = 1 kPa. Solid curves denote curve fits for non-linear regression models of normalized g_s − VPD (equation: normalized $g_s = a \times \ln(VPD) + b$). Dashed curves denote 95% prediction intervals of the regression models.

PV (peaked at 2 p.m.; Figure 4e). Among the species, PV usually had higher sunlit VPD_c than the other species—up to 0.3 kPa higher than both QA and QF (peaked at 5 p.m.)—except in the morning, where both QA (from 7 a.m. to 9 a.m.) and QF (from 8 a.m. to 1 p.m.) showed higher VPD_c than PV up to 0.2 kPa (both peaked at 8 a.m.).

Compared to the sunlit canopy portions, shaded portions always had lower VPD_c; the range of difference between sunlit VPD_c and shaded VPD_c during a day was 0.0–0.4 kPa for QA, 0.0–0.5 kPa for QF, and

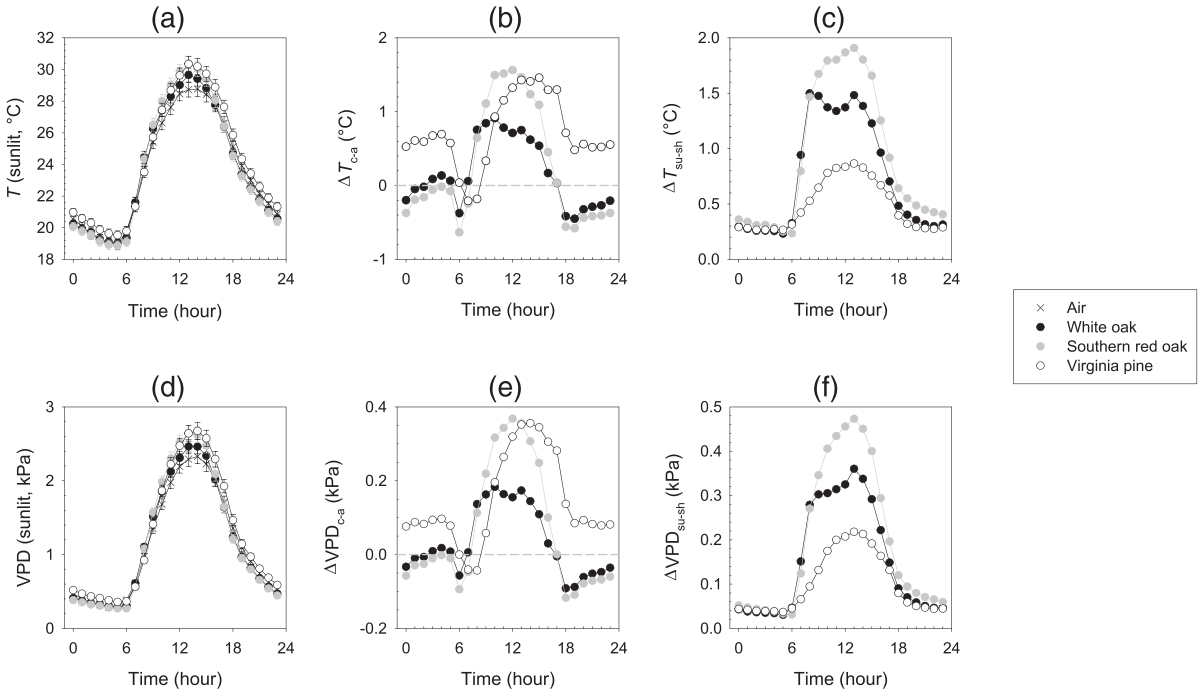

Figure 4. Mean diurnal variations of temperature (a) and VPD (d), the corresponding differences between sunlit canopy and air (b and e), and sunlit and shaded canopy portions (c and f) measurements for each species. Error bars represent standard errors of the means of hourly data (95% confidence). Horizontal dashed lines denote reference lines for $\Delta T = 0$ or $\Delta\mathrm{VPD} = 0$.

0.0–0.2 kPa for PV (Figure 4f). The difference was highest at 1 p.m. $\mathrm{VPD_c}$ for the shaded portions of QA and QF was always lower than $\mathrm{VPD_a}$ (up to 0.2 kPa for both species, peaking at both 7 a.m. and 6 p.m.) throughout the day. On the other hand, PV maintained higher $\mathrm{VPD_c}$ for the shaded portions than $\mathrm{VPD_a}$ at most times (up to 0.2 kPa, peaked at 2 p.m.), except a few hours in the morning (from 6 a.m. to 9 a.m.).

3.3. Species-Specific Response of T_c and $\mathrm{VPD_c}$ to Changing Condition

The response of $\Delta T_{c\text{-}a}$ to changing T_a was different across species (Figures 5a–5c). Specifically, PV maintained almost constant $\Delta T_{c\text{-}a}$ while the oak species had decreasing $\Delta T_{c\text{-}a}$ with rising T_a. The differences among the species were consistent in both sunlit and shaded canopy portions, with significantly lower $\Delta T_{c\text{-}a}$ for shaded portions than sunlit portions across the range of T_a ($p < 0.05$).

The differences among the species were more evident when the response of $\Delta\mathrm{VPD}_{c\text{-}a}$ to changing T_a was compared (Figures 5d–5f). In the case of sunlit canopy portions, QA consistently decreased $\Delta\mathrm{VPD}_{c\text{-}a}$ with rising T_a, while PV consistently increased $\Delta\mathrm{VPD}_{c\text{-}a}$. The response of QF to changing T_a was more or less constant. In the case of shaded portions, both QA and QF consistently decreased $\Delta\mathrm{VPD}_{c\text{-}a}$ with rising T_a, while the $\Delta\mathrm{VPD}_{c\text{-}a}$ of PV remained constant.

The species-specific differences were also apparent from the responses of $\Delta T_{c\text{-}a}$ and $\Delta\mathrm{VPD}_{c\text{-}a}$ to changing $\mathrm{VPD_a}$ (Figure 6). The differences among the species appears to be associated with species-specific stomatal regulation, and consequently, transpirational response (Figures 6g–6i); PV reduced J_s earlier at lower $\mathrm{VPD_a}$ than oak species, and leaf cooling did not completely offset leaf warming as shown in $\Delta T_{c\text{-}a}$ (Figures 6a–6c) and $\Delta\mathrm{VPD}_{c\text{-}a}$ responses (Figures 6d–6f).

4. Discussion

We investigated (1) species-specific responses of canopy temperature to changing air temperature or atmospheric dryness, and their associations with hydraulic traits, and (2) heterogeneities in canopy temperature across species and within a single canopy. The analysis leveraged continuous measurements using a TIC, which has not been widely applied for studies of tree canopies until recently (see Aubrecht et al., 2016,

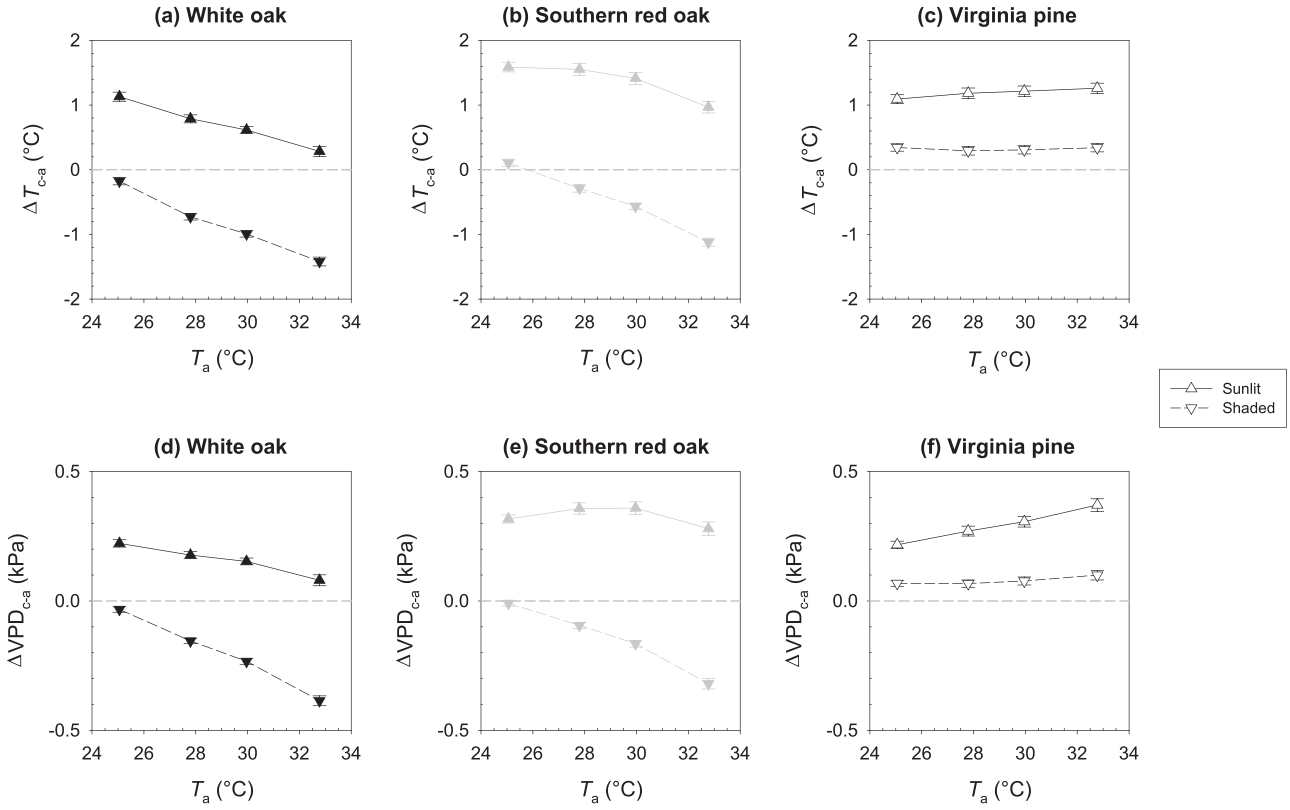

Figure 5. Δ $T_{c\text{-}a}$ (=$T_c - T_a$; a–c) and $\Delta VPD_{c\text{-}a}$ (=$VPD_c - VPD_a$; d–f) as functions of T_a. Note that the result is based on data collected during the daytime from 9 a.m. to 4 p.m. Each point represents mean value of samples from each bin of T_a. Error bars represent standard errors of the means (95% confidence). Horizontal dashed lines denote reference lines for $\Delta T_{c\text{-}a} = 0$ or $\Delta VPD_{c\text{-}a} = 0$.

and Kim et al., 2016, 2018, for earlier work). In the following sections, we discuss more details about a link between canopy temperature variability and plant hydraulic traits, its implications, and application of TICs.

4.1. Link Between Sensitivity in Canopy Temperature and Hydraulic Traits

One of our goals of the study was to understand how the T_c and VPD near the canopy surface are coordinated with species-specific stomatal regulation, that is, isohydricity. We found that T_c was notably higher than T_a for all observed species during the daytime, ranging from 1.0°C to 1.6°C (Figure 4b). The canopy was substantially cooled (relatively to T_a) under high T_a (Figure 5) and VPD_a (Figure 6) in white oak (QA) and southern red oak (QF) but less so in Virginia pine (PV), (Figure 4b). Moreover, it appears that the lower cooling effect of PV during the daytime persists into the nighttime (Figure 4b), imposing a higher heat load for most of the day, when compared to the other species. While it is not our research focus, understanding what limits net carbon uptake at high temperatures will become increasingly important since we are anticipating warmer climate in the near future.

The difference in T_c sensitivity among the species appears to be associated with hydraulic traits affecting stomatal regulation, and hence transpiration, in response to changing environmental conditions. Our diagnosis of species-specific hydraulic traits suggests that PV regulates stomatal conductance (g_s) more actively in response to changing moisture conditions (both soil moisture and atmospheric dryness) than QA and QF (Figure 3). Our identification of hydraulic traits agrees with previous studies identifying oak species as more anisohydric (Roman et al., 2015; Yi et al., 2019) and pine species as more isohydric species (Burkhardt & Pariyar, 2016; Klein et al., 2011).

The response of transpiration (represented by sap flux density, J_s) to changing moisture conditions was caused by stomatal regulation. The J_s of oak species persistently increased with rising VPD_a (Figures 6g and 6h) and decreasing soil moisture (Figure 2), due to their sustained g_s (note $J_s \propto g_s \cdot$ VPD given tree

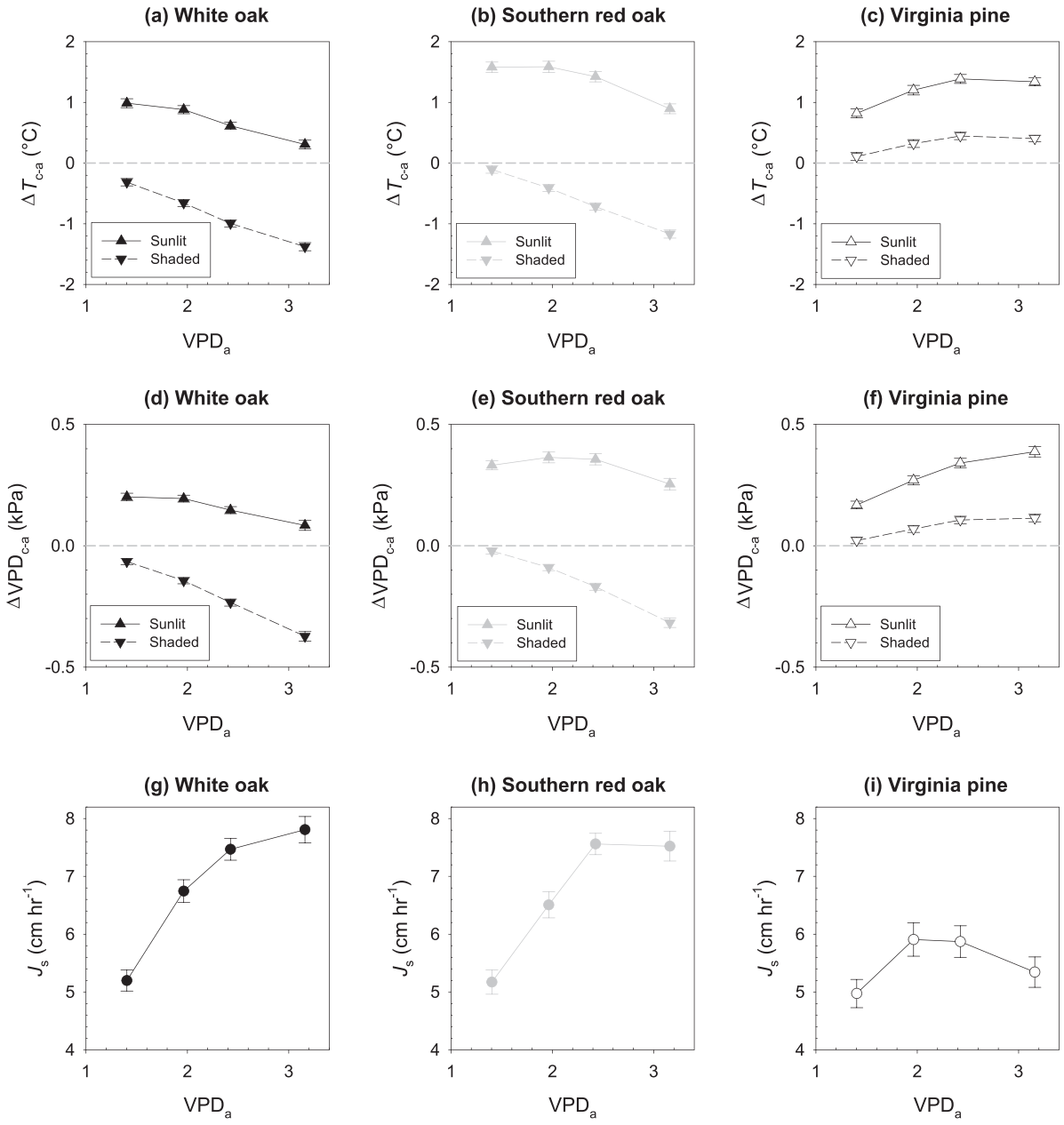

Figure 6. Δ $T_{c\text{-}a}$ (=T_c − T_a; a–c), $\Delta VPD_{c\text{-}a}$ (=VPD_c − VPD_a; d–f), and J_s (g–i) as functions of VPD_a. Note the result is based on data collected during the daytime from 9 a.m. to 4 p.m. Each point represents mean value of samples from each bin of T_a. Error bars represent standard errors of the means (95% confidence). Horizontal dashed lines denote reference lines for $\Delta T_{c\text{-}a} = 0$ or $\Delta VPD_{c\text{-}a} = 0$.

hydraulic conductivity and soil moisture are not limiting). Due to the higher cooling effect of oak species driven by higher transpiration rate under higher VPD_a, their heat (ΔT) and moisture (ΔVPD) stresses were reduced with increasing VPD_a. On the other hand, the J_s of PV saturated at a lower VPD_a (Figure 6i) and decreased when soil moisture was lower (Figure 2b), resulting in a less effective cooling effect than the oak species (e.g., sustained ΔT and increased ΔVPD with rising VPD_a; Figure 6). Overall, our results suggest that the oak species perform better in reducing the stresses from both increasing heat and dryness compared to the PV.

Meanwhile, it is important to consider the difference in rooting depth and soil moisture access among the species when diagnosing hydraulic traits. For instance, higher g_s of the oak species than the pine under

drier condition (Figure 3) can be attributed to their deeper rooting depth, which allows better access to moisture in the deeper soil when surface water is insufficient (Hochberg et al., 2018). Nonetheless, the impact of different soil moisture access among the species, if any, on our characterization of hydraulic traits is likely minimal. Throughout the study period, the VWC was fairly high without dropping below 0.25 m^3 m^{-3} within the soil depth of 30 cm. Moreover, our definition of dry soil conditions was relatively conservative considering almost 30% of cases were assumed to be dry. Despite the conservative definition, stomatal regulation of pine tree was clearly different from that of oak species. Therefore, we presume the difference in rooting depth and soil moisture access has little influence on the identification of hydraulic trait for the study species, at least for the relatively normal soil moisture regimes experienced during this study.

It was noteworthy that while using VPD_c (i.e., the VPD from a plant perspective) did not change our identification of hydraulic traits of the study species, VPD_c was significantly higher than VPD_a during the daytime (Figure 4e). Moreover, the sensitivity of g_s to VPD (i.e., the slope of g_s - VPD; Figure 3) was slightly overestimated when VPD_a was used instead of VPD_c, especially for the species that showed relatively large differences between T_c and T_a (QF and PV; Figure 4b). The difference in the slope was driven by the wider range of VPD_c than VPD_a, making the g_s-VPD_a slope lower (i.e., more negative) than the g_s-VPD_c slope (Figure 3). This implies that the g_s sensitivity to VPD is more likely to be overestimated when using VPD_a instead of VPD_c for more isohydric species like PV.

Our assumption for the difference between estimations of VPD_a and VPD_c was due to the choice of different temperature metrics (T_a vs. T_c) to calculate saturated vapor pressure of the air (vp_{sat} vs. $vp_{sat,canopy}$, Equations 2 and 4). However, one should note that VPD changes with *RH*, since actual vapor pressure of the air (vp_{air}; Equation 3) is a function of T_a and *RH*. While our T_a and *RH* were measured at a height similar to the tree height (Figure 1a), measured *RH* can be lower than actual *RH* at immediate proximity to the leaf surface due to better turbulent mixing of air, which can consequently result in smaller VPD_c than our estimation. Similarly, measured T_a can be different than T_a at immediate proximity to the leaf surface due to turbulent mixing of air and temperature gradient along the atmospheric layers. Although we assumed these micro-meteorological influences to be negligible, further leaf-level studies coupled with aerodynamics can help reduce the uncertainties we have discussed.

4.2. Other Factors Influencing Canopy Temperature Sensitivity

T_c can be also influenced by physical attributes of the leaves or canopy (leaf morphology or canopy structure). For instance, the large surface area per leaf of the oaks may allow their individual leaves to intercept more solar radiation than the pine needles do, resulting in their faster T_c increase in the morning (Figure 4b) when the difference in evaporative cooling effects among the species was relatively small (Figure 2). Meanwhile, lower canopy albedo for the pine canopy due to the darker hue of its needles (Juang et al., 2007) may contribute more positively to the T_c by absorbing and retaining heat better than the other species. This might have contributed to the high T_c of the pine tree in the afternoon and the retained high T_c even at night (Figure 4b). The different leaf warming effects among the species work independently from evaporative cooling effect, which complicates assessment of leaf thermoregulation: This is a major reason why we tested the relationship between evaporative cooling effect and canopy temperature indirectly by grouping data into different VPD_a (Figure 6), since VPD is directly associated with the leaf cooling mechanism (i.e., g_s regulation and J_s variability as a result) but not with warming effects. Therefore, comprehensive study including both warming and cooling factors together is required to clarify their impact on the leaf thermoregulation and its physiological consequence.

Additionally, more homogeneous T_c distribution of the pine (Figures 4c and 4f) may be attributable to its leaf morphology and foliage clumping, as these attributes result in more heterogeneous spatial distribution of leaf area within the canopy than typical broad-leaved trees (Cescatti, 1998). The heterogenous distribution of leaf area creates more gaps that allows higher canopy transmittance of solar radiation (Cescatti, 1998; Duursma & Mäkelä, 2007; Fotis & Curtis, 2017), making T_c distribution more homogenous within canopy. More homogenous spatial distribution of leaf area of the oak species, on the other hand, may cause the larger difference between sunlit and shaded T_c by intercepting solar radiation before it enters deeper into the canopy.

4.3. Implications of Variability in Cooling Effect Among Different Species

Among our studied species, PV showed large differences between T_c and T_a, and its sunlit T_c was up to 1.3°C higher than the oak species (Figure 4). This difference is notable considering the trees are co-occurring and experiencing almost identical environmental conditions. Furthermore, the difference in T_c among the species is comparable to the difference of surface temperature among different land covers/uses reported in other studies (~ +1°C in temperate zone by forest cover removal; Alkama & Cescatti, 2016; Bright et al., 2017). There are also relevant studies comparing surface temperature between co-located forests and grasslands in the eastern United States using radiometric measurements; for instance, Novick and Katul (2020) compared surface temperature (T_{surf}) of hardwood forest, pine forest, and grasslands using a radiometric approach and showed that T_{surf} of either type of the forests were cooler than the grassland (often exceeding 5°C) during the midday of a growing season. Zhang et al. (2020) reported that T_{surf} of grasslands was higher by 1–2°C than co-located forests at annual scale, with growing season temperature difference largely attributable to greater water use by forests.

One should note that, despite the notable difference in T_c across the co-occurring species, their cooling effect on T_c is not equal to the cooling effect on climate or T_a, which is more relevant for addressing climate mitigation roles of different vegetation types or species. While extending T_c or T_{surf} changes regulated by plants to T_a has been challenging due to the impact of heat transfer mechanism mediated by height of atmospheric boundary layer, Novick and Katul (2020) used a novel approach to assess the impact of reforestation on both T_a and T_{surf}. They showed that although the difference in T_a between forests and grassland was smaller than their difference in T_{surf}, T_a at the forests was 2–3°C cooler than the grassland during daytime growing season, which is still substantial.

Overall, despite the smaller cooling effect of vegetation on T_a than on T_c, evidence suggest that changes in species composition in forest ecosystems might cause changes in T_c that is comparable to the change caused by land use/cover change, which is likely to contribute to mitigate or aggravate global warming consequently. Our study species represent typical needleleaf and broadleaf trees that can be found in temperate forests in the eastern United States, and they are also typically known to be positioned very differently on the spectrum of hydraulic traits regarding their stomatal regulation. Specifically, oaks sustain stomatal opening under water stress (anisohydric; Roman et al., 2015; Yi et al., 2019) and pines as species closing stomata at earlier stages of water stress (isohydric; Burkhardt & Pariyar, 2016; Klein et al., 2011). A simple conjecture suggests that regions experiencing a shift in dominant species from anisohydric to isohydric (e.g., declined oak species in the eastern United States; Abrams, 2003; Flatley et al., 2013) might experience a reduction in the local cooling benefit provided by forested ecosystems. However, more work is needed to fully understand how species with contrasting hydraulic traits will respond to the warmer and drier conditions expected in the future. Moreover, vulnerability or mortality of iso/anisohydric species under those conditions is hard to generalize. Therefore, further advancement in on-going modeling efforts to incorporate plant hydraulic traits (e.g., SPAC model; Williams et al., 1996; Xu et al., 2016) into land surface models, along with more comprehensive understanding of plant thermoregulation in terms of energy balance and species-specific hydraulic traits, would inform the usefulness of reforestation as a local climate mitigation and adaptation strategy.

4.4. Thermal Imaging Camera as a Tool for Canopy Temperature Monitoring

High-resolution thermal images provide snapshots of the within- and cross-canopy heterogeneity in T_c. The TIC was ideal for T_c measurement of tall trees primarily due to its ability to overcome very low accessibility of tall-tree canopies. Unlike the infrared radiometers that record a single value of temperature per device, TIC can record temperatures at different parts of an image at the same time and allows visual inspection if the target was properly recorded, which enables partitioning sunlit and shaded portions within a canopy as shown in our study. Furthermore, being able to measure temperature of multiple positions from a single tree canopy means users can collect replication data for a single canopy at the same moment while all conditions are identically applied for those replications. This helps eliminate (1) biases that can arise otherwise, for instance, data collection at different times of similar conditions (but not exactly the same) to investigate plant-environment interactions, or (2) instrumental biases (e.g., positioning of instrument and synchronization of settings) that can arise from using separate instruments at the same time to measure different targets.

Therefore, the TIC has an advantage over infrared radiometers in recording temperature of targets with highly heterogeneous surfaces, while infrared radiometers should work well for targets with homogeneous surfaces (e.g., cropland).

We used the fixed ROIs to record mean T_c. The canopies were stationary under the most moderate conditions; however, canopies can sway when wind is high. Although the positions for ROIs were carefully chosen to always properly target the canopies considering the trajectories of canopy movements, developing an algorithm to track the movement of targets and measuring them might improve the results. Nevertheless, our measurements were highly precise with very low variations (e.g., low standard errors throughout the results; also see Figure S2 in the supporting information showing a result from preliminary test performed on multiple leaves of a plant growing in the pot), suggesting the use of fixed targets can still provide reliable measurements if their positions are carefully set.

5. Conclusion

We found notable differences among the study species in the sensitivities of canopy temperature (T_c) and VPD at the canopy surface (VPD_c) to rising air temperature (T_a) and atmospheric water demand (VPD_a), which was closely related to species-specific hydraulic traits. Specifically, the isohydric species, which regulated stomatal conductance more strongly under conditions of drier soil moisture, experienced larger differences between T_c and T_a. It is noteworthy that the variability of sunlit T_c among the species was up to 1.3°C, which was comparable to the surface temperature variation caused by land use change reported elsewhere (1°C to 2°C). This implies that change in species composition can have a significant impact on the local to regional surface temperature. Meanwhile, we also found the heterogeneity of T_c within the canopy (from the difference between sunlit and shaded T_c) can be remarkably different depending on the species, which may be attributed to their different leaf and canopy structure. Therefore, more precise evaluation of the feedback between plant thermoregulation and climate system would benefit from the improved and comprehensive understanding of plant hydraulic traits and energy exchange processes occurring at both canopy-atmosphere interface and within the canopy.

Data Availability Statement

Data used in this study are available on Zenodo (https://doi.org/10.5281/zenodo.3896812).

Acknowledgments

K. Y., X. Y., and M. L. acknowledge support from the National Science Foundation (NSF) through Division of Integrative Organismal Systems (grant 2005574). K. Y., X. Y., T. M. S., and M. L. acknowledge support from the NSF Division of Atmospheric and Geospace Sciences (grant 1837891). K. Y. and X. Y. acknowledge support from the National Aeronautics and Space Administration (grant 80NSSC17K0110) and Center for Innovative Technology through Commonwealth Research Commercialization Fund (grant MF20-008-US_UVA). K. N. acknowledges support from the NSF Division of Environmental Biology (grant 1552747).

References

Abrams, M. D. (2003). Where has all the white oak gone? *Bioscience*, *53*(10), 927–939. https://doi.org/10.1641/0006-3568(2003)053[0927:WHATWO]2.0.CO;2

Alkama, R., & Cescatti, A. (2016). Climate change: Biophysical climate impacts of recent changes in global forest cover. *Science*, *351*(6273), 600–604. https://doi.org/10.1126/science.aac8083

Aubrecht, D. M., Helliker, B. R., Goulden, M. L., Roberts, D. A., Still, C. J., & Richardson, A. D. (2016). Continuous, long-term, high-frequency thermal imaging of vegetation: Uncertainties and recommended best practices. *Agricultural and Forest Meteorology*, *228-229*, 315–326. https://doi.org/10.1016/j.agrformet.2016.07.017

Berry, J., & Bjorkman, O. (1980). Photosynthetic response and adaptation to temperature in higher plants. *Annual Review of Plant Physiology*, *31*(1), 491–543. https://doi.org/10.1146/annurev.pp.31.060180.002423

Blonquist, J. M., Norman, J. M., & Bugbee, B. (2009). Automated measurement of canopy stomatal conductance based on infrared temperature. *Agricultural and Forest Meteorology*, *149*(12), 2183–2197. https://doi.org/10.1016/j.agrformet.2009.10.003

Bright, R. M., Davin, E., O'Halloran, T., Pongratz, J., Zhao, K., & Cescatti, A. (2017). Local temperature response to land cover and management change driven by non-radiative processes. *Nature Climate Change*, *7*(4), 296–302. https://doi.org/10.1038/nclimate3250

Burgess, S. S. O., Adams, M. A., Turner, N. C., Beverly, C. R., Ong, C. K., Khan, A. A. H., & Bleby, T. M. (2001). An improved heat pulse method to measure low and reverse rates of sap flow in woody plants. *Tree Physiology*, *21*(9), 589–598. https://doi.org/10.1093/treephys/21.9.589

Burkhardt, J., & Pariyar, S. (2016). How does the VPD response of isohydric and anisohydric plants depend on leaf surface particles? *Plant Biology*, *18*(S1), 91–100. https://doi.org/10.1111/plb.12402

Cescatti, A. (1998). Effects of needle clumping in shoots and crowns on the radiative regime of a Norway spruce canopy. *Annales Des Sciences Forestieres*, *55*(1–2), 89–102. https://doi.org/10.1051/forest:19980106

Chan, W. Y. S. (2011). *The fate of biogenic hydrocarbons within a forest canopy: Field observations and model results* (Doctoral dissertation). Charlottesville, VA: University of Virginia. Retrieved fromProQuest Dissertations Publishing (https://www.proquest.com/docview/905174469?accountid=14678)

Duursma, R. A., & Mäkelä, A. (2007). Summary models for light interception and light-use efficiency of non-homogeneous canopies. *Tree Physiology*, *27*(6), 859–870. https://doi.org/10.1093/treephys/27.6.859

Fei, S., Kong, N., Steiner, K. C., Moser, W. K., & Steiner, E. B. (2011). Change in oak abundance in the eastern United States from 1980 to 2008. *Forest Ecology and Management*, *262*(8), 1370–1377. https://doi.org/10.1016/j.foreco.2011.06.030

Ficklin, D. L., & Novick, K. A. (2017). Historic and projected changes in vapor pressure deficit suggest a continental-scale drying of the United States atmosphere. *Journal of Geophysical Research: Atmospheres*, *122*, 2061–2079. https://doi.org/10.1002/2016JD025855

Flatley, W. T., Lafon, C. W., Grissino-Mayer, H. D., & LaForest, L. B. (2013). Fire history, related to climate and land use in three southern Appalachian landscapes in the eastern United States. *Ecological Applications*, *23*(6), 1250–1266. https://doi.org/10.1890/12-1752.1

Fotis, A. T., & Curtis, P. S. (2017). Effects of structural complexity on within-canopy light environments and leaf traits in a northern mixed deciduous forest. *Tree Physiology*, *37*(10), 1426–1435. https://doi.org/10.1093/treephys/tpw124

Gimenez, B. O., Jardine, K. J., Higuchi, N., Negrón-Juárez, R. I., Sampaio-Filho, I. d. J., Cobello, L. O., et al. (2019). Species-specific shifts in diurnal sap velocity dynamics and hysteretic behavior of ecophysiological variables during the 2015–2016 El Niño event in the amazon forest. *Frontiers in Plant Science*, *10*, 830. https://doi.org/10.3389/fpls.2019.00830

Greer, D. H., & Weedon, M. M. (2012). Modelling photosynthetic responses to temperature of grapevine (*Vitis vinifera* cv. Semillon) leaves on vines grown in a hot climate. *Plant, Cell and Environment*, *35*(6), 1050–1064. https://doi.org/10.1111/j.1365-3040.2011.02471.x

Grossiord, C., Buckley, T. N., Cernusak, L. A., Novick, K. A., Poulter, B., Siegwolf, R. T. W., et al. (2020). Plant responses to rising vapor pressure deficit. *New Phytologist*, *226*(6), 1550–1566. https://doi.org/10.1111/nph.16485

Helliker, B. R., & Richter, S. L. (2008). Subtropical to boreal convergence of tree-leaf temperatures. *Nature*, *454*(7203), 511–514. https://doi.org/10.1038/nature07031

Hochberg, U., Rockwell, F. E., Holbrook, N. M., & Cochard, H. (2018). Iso/anisohydry: A plant-environment interaction rather than a simple hydraulic trait. *Trends in Plant Science*, *23*(2), 112–120. https://doi.org/10.1016/j.tplants.2017.11.002

Intergovernmental Panel on Climate Change (IPCC) (2018). Summary for policymakers. In V. Masson-Delmotte, et al. (Eds.), *Global warming of 1.5°C. An IPCC Special Report on the impacts of global warming of 1.5°C above pre-industrial levels and related global greenhouse gas emission pathways, in the context of strengthening the global response to the threat of climate change, sustainable development, and efforts to eradicate poverty*. Geneva, Switzerland: World Meteorological Organization. https://www.ipcc.ch/sr15/chapter/spm/

Jones, H. G. (2004). Application of thermal imaging and infrared sensing in plant physiology and ecophysiology. *Advances in Botanical Research*, *41*, 107–163. https://doi.org/10.1016/s0065-2296(04)41003-9

Juang, J. Y., Katul, G., Siqueira, M., Stoy, P., & Novick, K. (2007). Separating the effects of albedo from eco-physiological changes on surface temperature along a successional chronosequence in the southeastern United States. *Geophysical Research Letters*, *34*, L21408. https://doi.org/10.1029/2007GL031296

Kim, Y., Still, C. J., Hanson, C. V., Kwon, H., Greer, B. T., & Law, B. E. (2016). Canopy skin temperature variations in relation to climate, soil temperature, and carbon flux at a ponderosa pine forest in central Oregon. *Agricultural and Forest Meteorology*, *226-227*, 161–173. https://doi.org/10.1016/j.agrformet.2016.06.001

Kim, Y., Still, C. J., Roberts, D. A., & Goulden, M. L. (2018). Thermal infrared imaging of conifer leaf temperatures: Comparison to thermocouple measurements and assessment of environmental influences. *Agricultural and Forest Meteorology*, *248*, 361–371. https://doi.org/10.1016/j.agrformet.2017.10.010

Klein, T., Cohen, S., & Yakir, D. (2011). Hydraulic adjustments underlying drought resistance of *Pinus halepensis*. *Tree Physiology*, *31*(6), 637–648. https://doi.org/10.1093/treephys/tpr047

Leuzinger, S., & Körner, C. (2007). Tree species diversity affects canopy leaf temperatures in a mature temperate forest. *Agricultural and Forest Meteorology*, *146*(1–2), 29–37. https://doi.org/10.1016/j.agrformet.2007.05.007

Leuzinger, S., Vogt, R., & Körner, C. (2010). Tree surface temperature in an urban environment. *Agricultural and Forest Meteorology*, *150*(1), 56–62. https://doi.org/10.1016/j.agrformet.2009.08.006

Mahan, J. R., & Upchurch, D. R. (1988). Maintenance of constant leaf temperature by plants—I. Hypothesis-limited homeothermy. *Environmental and Experimental Botany*, *28*(4), 351–357. https://doi.org/10.1016/0098-8472(88)90059-7

McDowell, N., Pockman, W. T., Allen, C. D., Breshears, D. D., Cobb, N., Kolb, T., et al. (2008). Mechanisms of plant survival and mortality during drought: Why do some plants survive while others succumb to drought? *New Phytologist*, *178*(4), 719–739. https://doi.org/10.1111/j.1469-8137.2008.02436.x

Monteith, J. L., & Unsworth, M. H. (2014). *Principles of environmental physics: Plants, animals, and the atmosphere* (4th ed.). Waltham, MA: Academic Press. https://doi.org/10.1016/C2010-0-66393-0

Novick, K. A., Ficklin, D. L., Stoy, P. C., Williams, C. A., Bohrer, G., Oishi, A. C., et al. (2016). The increasing importance of atmospheric demand for ecosystem water and carbon fluxes. *Nature Climate Change*, *6*(11), 1023–1027. https://doi.org/10.1038/Nclimate3114

Novick, K. A., & Katul, G. G. (2020). The duality of reforestation impacts on surface and air temperature. *Journal of Geophysical Research: Biogeosciences*, *125*, e2019jg005543. https://doi.org/10.1029/2019JG005543

Oren, R., Sperry, J. S., Katul, G. G., Pataki, D. E., Ewers, B. E., Phillips, N., & Schafer, K. V. R. (1999). Survey and synthesis of intra- and interspecific variation in stomatal sensitivity to vapour pressure deficit. *Plant, Cell & Environment*, *22*(12), 1515–1526. https://doi.org/10.1046/j.1365-3040.1999.00513.x

Roman, D. T., Novick, K. A., Brzostek, E. R., Dragoni, D., Rahman, F., & Phillips, R. P. (2015). The role of isohydric and anisohydric species in determining ecosystem-scale response to severe drought. *Oecologia*, *179*(3), 641–654. https://doi.org/10.1007/s00442-015-3380-9

Williams, M., Rastetter, E. B., Fernandes, D. N., Goulden, M. L., Wofsy, S. C., Shaver, G. R., et al. (1996). Modelling the soil-plant-atmosphere continuum in a *Quercus-Acer* stand at Harvard forest: The regulation of stomatal conductance by light, nitrogen and soil/plant hydraulic properties. *Plant, Cell and Environment*, *19*(8), 911–927. https://doi.org/10.1111/j.1365-3040.1996.tb00456.x

Xu, X., Medvigy, D., Powers, J. S., Becknell, J. M., & Guan, K. (2016). Diversity in plant hydraulic traits explains seasonal and inter-annual variations of vegetation dynamics in seasonally dry tropical forests. *New Phytologist*, *212*(1), 80–95. https://doi.org/10.1111/nph.14009

Yi, K., Maxwell, J. T., Wenzel, M. K., Roman, D. T., Sauer, P. E., Phillips, R. P., & Novick, K. A. (2019). Linking variation in intrinsic water-use efficiency to isohydricity: A comparison at multiple spatiotemporal scales. *New Phytologist*, *221*(1), 195–208. https://doi.org/10.1111/nph.15384

Zhang, Q., Barnes, M., Benson, M., Burakowski, E., Oishi, A. C., Ouimette, A., et al. (2020). Reforestation and surface cooling in temperate zones: Mechanisms and implications. *Global Change Biology*, *26*(6), 3384–3401. https://doi.org/10.1111/gcb.15069

Zhao, K., & Jackson, R. B. (2014). Biophysical forcings of land-use changes from potential forestry activities in North America. *Ecological Monographs*, *84*(2), 329–353. https://doi.org/10.1890/12-1705.1